T_c of the Mode Coupling Theory Evaluated from Impulsive Stimulated Light Scattering on Salol

Yongwu Yang and Keith A. Nelson
Department of Chemistry, Massachusetts Institute of Technology, Cambridge, Massachusetts 02139

(Received 2 November 1994)

Time-domain light scattering on ns–ms time scales has been performed on salol to probe the dynamics in the glass transition range and evaluate through a novel method the nonergodicity parameter $f_q(T)$ of mode coupling theory (MCT) in the wave vector limit $q \to 0$. Stretched-exponential structural relaxation dynamics were observed. In addition, a cusp in $f_0(T)$ was observed at a temperature T_c of ~266 K, consistent with earlier observations at high q. This supports the MCT prediction of a cusp at a q-independent temperature.

PACS numbers: 64.70.Pf, 65.70.+y, 78.47.+p

Much recent experimental research on the liquid-glass transition has been focused on the dynamics in fragile liquids in order to test various predictions of mode coupling theory (MCT). The most prominent feature of the dynamics is strongly temperature-dependent structural relaxation, referred to as the α relaxation, in supercooled liquids. The α relaxation generally obeys over a rather wide time range the Kohlrausch-Williams-Watts (KWW) relaxation function $\phi(t) = A\exp\{-(t/\tau)^\beta\}$, with $0 < \beta \leq 1$ describing the degree of nonexponentiality. The dynamics often span several decades of temporal range at a single temperature and on the order of thirteen decades as the temperature is varied, so a very wide dynamic range is required for critical examination of the α relaxation structure.

A central result of MCT is the prediction of a crossover temperature T_c at which the Debye-Waller factor $f_q(T)$, defined as the integrated area of the α peak, shows a square-root cusp [1]:

$$f_q(T) = \begin{cases} f_q^c & (T > T_c), \\ f_q^c + h_q[(T_c - T)/T_c]^{1/2} & (T < T_c), \end{cases} \quad (1)$$

where f_q^c is a slowly varying function of T. Although the value of $f_q(T)$ is q dependent, the crossover temperature should not depend on wave vector.

Equation (1) has been shown to be consistent with the results of neutron scattering experiments for several materials [1]. In the low-q limit $f_q(T)$ can be determined through polarized Rayleigh-Brillouin scattering (BS) through the relation [2] which has been shown to hold irrespective of the form of the relaxation function [3,4]:

$$f_0 = 1 - (c_0/c_\infty)^2, \quad (2)$$

where c_∞ (c_0) is the limiting sound velocity measured above (below) the α relaxation frequency range. However, due to the limited wave vector and frequency range usually examined, BS spectra generally do not permit accurate characterization of the α relaxation (i.e., Mountain) mode [5] over a temperature range sufficient for unique determination of T_c through Eq. (1). Thus the BS value of T_c determined for propylene carbonate [6] exceeded that determined through neutron scattering [7] by 60 K. In other cases [4,8], BS spectra have not been used for a unique determination but have been found to be consistent with values of T_c determined through neutron scattering measurements of $f_q(T)$ and depolarized light scattering (DLS) susceptibility spectra (which provide a separate, dynamical route to T_c, not involving the Debye-Waller factor). More tests of Eq. (1) are clearly necessary, especially in the low-q limit which is currently inaccessible.

In order to test Eq. (1) for the behavior of f_0 and possible q dependence of T_c, we have performed a study of the glass-forming liquid salol (phenyl salicylate, $T_g = 218$ K, $T_m = 315$ K) through impulsive stimulated thermal scattering (ISTS). In this Letter we present observations of structural relaxation spanning a time range of 6 decades (from ns to ms) and a square-root cusp in the Debye-Waller factor.

ISTS has been used to study the dynamics of various glass-forming materials over the last several years [9,10]. The experiments reported here were performed with a modified quasi-cw probe system which allows us to collect data with far higher signal/noise and over a far wider temporal range (from ns to ms) than previously. Two 100-ps, parallel polarized laser pulses at excitation wavelength $\lambda_E = 1.064$ μm are crossed at an angle θ_E and form an intensity interference pattern with wave vector magnitude $q = (4\pi/\lambda_E)\sin(\theta_E/2)$. Optical absorption at the intensity peaks and the fast nonradiative decay give rise to a temperature grating and, through thermal expansion, a time-dependent density response with the same wave vector q. This response is monitored through time-resolved diffraction of a quasi-cw probe light. The entire temporal response, which may be monitored out to millisecond or longer time scales, is recorded in a single laser shot. Typically, about 1000 shots are averaged over a total data acquisition time of about 10 s.

ISTS probes the time-dependent density response to sudden, spatially periodic heating. Starting from the generalized hydrodynamics equations with a single-relaxation-time process [5,11], one can derive the density response function $G_{\rho T}(q,t)$ [12] measured in ISTS as

$$I(q,t) = |G_{\rho T}(q,t)|^2 = \Big\{A\Big[e^{-\Gamma_H t} - e^{-\Gamma_A t}\cos(\omega_A t)\Big] + B\Big[e^{-\Gamma_H t} - e^{-(\Gamma_R t)^{\beta}}\Big]\Big\}^2, \quad (3)$$

with $\beta = 1$, where Γ_H is the thermal decay rate and Γ_A and ω_A are the acoustic attenuation rate and frequency, respectively. The response consists of two parts. The first "A" term describes the behavior of simple liquids, including glass-forming liquids at high temperatures. In such samples, sudden spatially periodic heating at wave vector q leads to spatially periodic thermal expansion which occurs on the time scale of half the acoustic oscillation period $\pi/\omega_A(q)$. There are a transient acoustic response consisting of damped acoustic oscillations and a steady-state density modulation which decays due to thermal diffusion at rate $\Gamma_H(q)$. These are time-domain observations of the Brillouin and Rayleigh features in the light scattering spectrum. The second "B" term describes the modifications to this behavior for viscoelastic fluids. Then density response still has the A term, which includes acoustic oscillations, but also a slower nonoscillatory rise which might be described well by the KWW function with characteristic relaxation time and stretching exponent Γ_R^{-1} and β, respectively. This is a time-domain observation of the relaxation or Mountain mode. Only at low temperatures, when structural relaxation dynamics (i.e., the time-dependent rise in signal) become slow compared to thermal diffusion [i.e., $\Gamma_R \leq \Gamma_H(q)$] does overlap of the Mountain and Rayleigh contributions present a problem. However, ISTS experiments are practical with very small scattering angles (less than 0.5°) at which the (q^2-dependent) thermal diffusion dynamics can be slowed considerably to permit accurate characterization of the (q-independent) gradual rise. At high temperatures, the structural relaxation dynamics eventually become fast compared to an acoustic oscillation period [i.e., $\Gamma_R \geq \omega_A(q)$] which defines the limit of how fast the sample density can respond to sudden heating or stress at wave vector q. At such temperatures the rise in signal is limited only by the acoustic period, and structural relaxation dynamics which are faster than this cannot be observed. However, the acoustic period can be shortened by going to large scattering angles, thereby extending to higher T the range over which the relaxation mode can be characterized.

In summary, the manifestations of Rayleigh, Mountain, and acoustic features in ISTS data and the wide wave vector range accessible to ISTS yield a substantial range of temperatures over which q values can be reached such that the relations $\Gamma_R \ll \omega_A$ and $\Gamma_R \gg \Gamma_H$ hold and the Mountain mode can be well characterized. In this case the solution to the generalized hydrodynamic equations leads to an important result [12] about the relative signal amplitudes due to structural relaxation and thermal mode:

$$B/(A + B) = 1 - (c_0/c_\infty)^2. \quad (4)$$

Through ISTS data and Eqs. (4) and (2), and alternate pathway is provided for determination of $f_q(T)$ in the low-q limit and thus for testing of the MCT prediction in Eq. (1). It can be shown [12] that this does not depend on the particular choice of relaxation function. Thus it holds for the KWW function with $1 > \beta > 0$ or other forms. Thinking of the normalized (i.e., $A + B = 1$) ISTS response function in the frequency domain, Eqs. (4) and (2) state that when the Mountain, Rayleigh, and acoustic peaks are well separated from each other, the integrated area of the Mountain mode gives $f_0(T)$, which is natural result of the definition of Debye-Waller factor.

Note that Eqs. (3) and (4) would need modification if β relaxation processes were slow enough to contribute to the gradual rise observed on nanosecond time scales in the ISTS signal. Since all available evidence [13(a),(b)] suggests that β relaxation in molecular liquids occurs on picosecond time scales at $T > T_g$, its contribution can be reasonably neglected.

In Fig. 1 we show the raw data (solid curves) and fits (dotted curves) by Eq. (3) for temperatures from 268

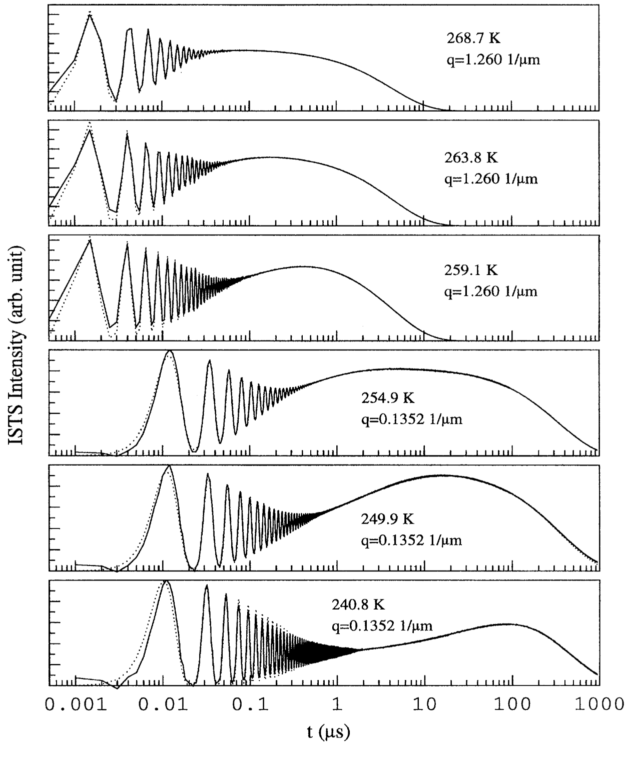

FIG. 1. ISTS date (solid curves) and fits (dotted curves) by Eq. (3) of salol at several temperatures. Signal shows damped acoustic oscillations, and reaches a steady-state level rapidly at high temperatures and more slowly (due to slow structural relaxation or Mountain mode) at low temperatures. Signal decays at long times due to thermal diffusion.

to 240 K. Excellent fits to data permit determination of the dynamical parameters Γ_H, Γ_A, and ω_A (as well as Γ_R and β) and the relative amplitudes of A and B. The acoustic and thermal responses given by these parameters were then subtracted from the square root of the raw data. The relaxation function $\phi(t;T)$ which remains (solid curves of Fig. 2) was fit again with the KWW function (dotted curves), yielding values of Γ_R and β which in all cases agreed well with those from the original fits. It is evident from Fig. 2 that upon increasing temperature the relaxation shifts toward shorter times. For $T > 300$ K, it is no longer detectable because the relaxation time is shorter than half the acoustic oscillation period at the highest q reached. For $T \geq 285$ K, the relaxation response is detectable but too fast to permit reliable determination of the relaxation parameters Γ_R and β or the amplitude ratio A/B. Between 275 and 285 K, the Mountain contribution is slow enough that its amplitude could be measured reliably even though its dynamics are not determined uniquely. We fixed the two parameters Γ_R and β at values found through DLS [13(a)] and determined the amplitude ratio A/B. As a check, β was fixed exceeds the uncertainty range of our own measurements, and τ and A/B were allowed to vary. The result produced little variation in the value of A/B. Below 238 K, the relaxation dynamics are comparable to or slower then thermal diffusion times even at the smallest q used, and we could not obtain the relaxation function or the amplitude ratio reliably.

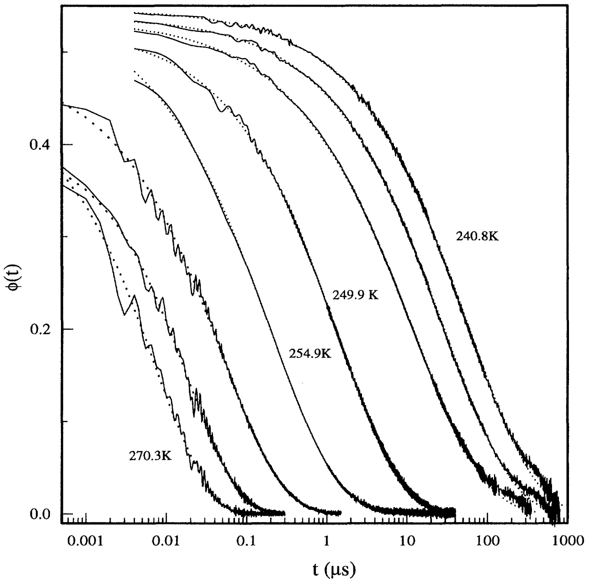

FIG. 2. Salol structural relaxation functions $\phi(t;T)$ (solid curves) extracted from ISTS data at 240.8, 242.8, 244.8, 249.9, 254.9, 260.1, 265.3, and 270.3 K. KWW fits (dotted curves) are also shown. Upon increasing temperature the relaxation dynamics become faster.

The average relaxation times $\langle\tau\rangle$ are plotted in Fig. 3 for several wave vectors from this study, together with $\langle\tau\rangle$ values from DLS [13(a)] and photon correlation spectroscopy (PCS) [14]. Data from ISTS cover the gap between PCS and DLS measurements and show a smooth variation in $\langle\tau\rangle$ between the two. The β values from this study, plotted in the inset of Fig. 3, are essentially constant at 0.52 ± 0.03 in the temperature range of 238–261 K and then increase at higher T. Very similar results were observed in dielectric measurements [15], with the increase in β at the same temperature range. MCT does not offer quantitative predictions for β at $T \leq T_c$, but numerical calculations [16] indicate that β may change significantly near T_c.

Because Eq. (4) is valid only when $\omega_A(q;T) \gg \Gamma_R(T) \gg T_H(q;T)$, we chose $\Gamma_R(T) \geq 10\Gamma_H(q;T)$ and $\Gamma_R(T) \leq 10\omega_A(q;T)$ as criteria for determination of $f_0(T)$ values from fitting parameters via Eqs. (4) and (2) in the temperature range from each wave vector. The resulting $f_0(T)$ values (symbols) are plotted in Fig. 4, where the solid line is a fit by Eq. (1). The fitting parameters are $f_0^c = 0.36 \pm 0.01$, $h_0 = 0.52 \pm 0.05$, and $T_c = 266.1 \pm 0.5$ K. This T_c value is in good agreement with neutron scattering results of $T_c = 263 \pm 7$ K at $q = 1.5$ and 1.0 Å^{-1} [17], which confirms q-independent T_c through Eq. (1). This result is also consistent with the previous determination $T_c = 256 \pm 5$ K from DLS [13(a)].

In summary, we have presented a novel determination of the Debye-Waller factor and test of the MCT through time-domain ISTS observations of slow structural relaxation in salol. A cusp in the T-dependent Debye-Waller

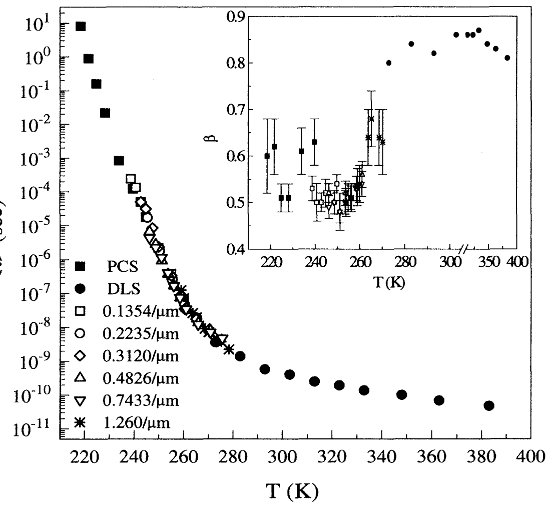

FIG. 3. Temperature dependence of $\langle\tau\rangle$ from the present ISTS data, previous depolarized light scattering, and photon correlation spectroscopy. Data from ISTS cover the gap between DLS and PCS and form a smooth curve. Inset shows the β values from ISTS, DLS, and PCS vs T. β values below 261 K from this study are essentially temperature independent.

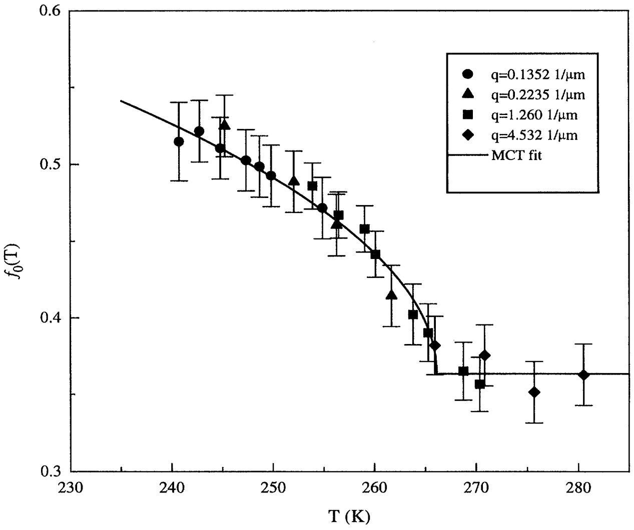

FIG. 4. Debye-Waller factor $f_0(T)$ (symbols) of salol vs T. The solid curve represents the fit by Eq. (1). The uncertainties indicated in the plot are the results of using different values of β within their uncertainty ranges.

factor is observed. The result is in good agreement with the MCT prediction of q-independent T_c and with other measurements at high and low wave vectors.

This work was supported in part by NSF Grant No. DMR-9317198 and by the donors of the Petroleum Research Fund, administered by the American Chemical Society.

[1] W. Gotze and L. Sjogren, Rep. Prog. Phys. **55**, 241 (1992).

[2] M. Fuchs, W. Gotze, and A. Latz, Chem. Phys. **149**, 185 (1990).

[3] W. Gotze, in *Phase Transitions and Relaxation in Systems with competing Energy Scales,* edited by T. Riste and D. Sherrington (Kluwer, Netherlands, 1993), p. 191.

[4] G. Li, M. Du, J. Hernandez, and H. Z. Cummins, Phys. Rev. E **48**, 1192 (1993).

[5] R. D. Mountain, J. Res. Natl. Bur. Stand. Sect. A **70**, 207 (1966).

[6] M. Elmroth, L. Borjesson, and L. M. Torell, Phys. Rev. Lett. **68**, 79 (1992).

[7] L. Borjesson, M. Elmroth, and L. M. Torell, Chem. Phys. **149**, 209 (1990).

[8] C. Dreyfus *et al.,* Phys. Rev. Lett. **69**, 3666 (1992).

[9] (a) Y.-X. Yan, L.-T. Cheng, and K. A. Nelson, J. Chem. Phys. **88**, 6477 (1988); (b) A. R. Duggal and K. A. Nelson, *ibid.* **94**, 7677 (1991); (c) S. M. Silence, A. R. Duggal, L. Dhar, and K. A. Nelson, *ibid.* **96**, 5448 (1992); (d) I. Halalay and K. A. Nelson, *ibid.* **97**, 3557 (1992). Note that the expression for $G_{\rho T}(q,t)$ in (b) differs from Eq. (3) of the text in that the thermal mode contribution to the second B term was not accounted for properly.

[10] I. C. Halalay, Y. Yang, and K. A. Nelson, J. Non-Cryst. Solids **172–174**, 175 (1994).

[11] J. P. Boon and S. Yip, *Molecular Hydrodynamics* (McGraw-Hill, New York, 1980).

[12] Y. Yang and K. A. Nelson (to be published).

[13] (a) G. Li, W. M. Du, A. Sakai, and H. Z. Cummins, Phys. Rev. A **46**, 3343 (1992); (b) W. M. Du *et al.,* Phys. Rev. E **49**, 2192 (1994).

[14] D. L. Sidebottom and C. M. Sorensen, Phys. Rev. B **40**, 461 (1989).

[15] P. K. Dixon, L. Wu, S. R. Nagel, B. D. Williams, and J. P. Carini, Phys. Rev. Lett. **65**, 1108 (1990).

[16] W. Gotze and L. Sjogren, J. Phys. C **21**, 3407 (1988).

[17] J. Toulouse, G. Coddens, and R. Pattnaik, Physica (Amsterdam) **201A**, 305 (1993).